

Filling distribution gaps: Two new species of the catfish genus *Cambeva* from southern Brazilian Atlantic Forest (Siluriformes, Trichomycteridae)

Wilson J. E. M. Costa¹, Caio R. M. Feltrin², Axel M. Katz¹

¹ *Laboratory of Systematics and Evolution of Teleost Fishes, Institute of Biology, Federal University of Rio de Janeiro, Caixa Postal 68049, CEP 21941-971, Rio de Janeiro, Brazil*

² *Av. Municipal, 45, Siderópolis, CEP 88860-000, Santa Catarina, Brazil*

<http://zoobank.org/FCED0DBF-90AA-4299-B3C3-8B208971EBA6>

Corresponding author: Wilson J. E. M. Costa (wcosta@acd.ufrj.br)

Academic editor: Nicolas Hubert ♦ Received 21 November 2020 ♦ Accepted 25 January 2021 ♦ Published 2 March 2021

Abstract

The fauna and flora of the Brazilian Atlantic Forest have been intensively inventoried since the 19th century, but some components of this rich biota are still poorly known, and some areas have been poorly sampled. Recent studies on a rich collection of mountain catfishes of the genus *Cambeva* have revealed a high diversity of species still undescribed in the region. Here we provide formal descriptions for two of these species, found in areas inserted in a broad gap of the presently known genus distribution. The first one is endemic to small coastal river basins of Santa Catarina state, southern Brazil; it is tentatively placed in an intrageneric clade, also including *C. castroi*, *C. davisii*, *C. guareiensis* and *C. zonata*, by all sharing the presence of a flat small process on the dorsal margin of the quadrate, laterally overlapping metapterygoid and situated just posterior to the syncondrial joint between the metapterygoid and the quadrate. Phylogenetic relationships of the second new species, endemic to the Rio Itajaí-Mirim basin, are still obscure, but it shares a derived morphology of the mesethmoid with some species of the *C. balios* group. Although species of *Cambeva* have little external morphological variation when compared to other trichomycterine groups, the present study once more shows the importance of recording and using osteological characters to diagnose externally similar trichomycterine species.

Key Words

Comparative morphology, mountain biodiversity, osteology, systematics

Introduction

The fauna and flora of the Brazilian Atlantic Forest, considered among the most important biodiversity hotspots in the world (Myers et al. 2000), have been intensively inventoried and described since the first half of the 19th century, when numerous European naturalists visited the region for the first time (e.g. Papavero 1971; Costa et al. 2020a). However, after about 200 years of regular studies, some components of this rich biota are still poorly known. Among freshwater fishes, represented in streams of this region by over 270 species (e.g. Abilhoa et al. 2011), studies based on expeditions conducted in the last

30 years directed to sample fish in specialised biotopes have revealed a rich still unknown species diversity, first described in recent years (e.g. Costa 2009; Costa et al. 2020b). Among these specialised freshwater biotopes are mountain streams, with numerous endemic fishes being first sampled and described in recent years, mainly belonging to the Trichomycterinae (Costa et al. 2020c, 2020d; Donin et al. 2020; dos Reis et al. 2020; Vilarido et al. 2020), a catfish subfamily (Siluriformes: Trichomycteridae) occurring between southern Central America and Patagonia, in southern South America (Katz et al. 2018).

Trichomycterines are typically found in fast-flowing streams and each species is usually geographically re-

stricted to small areas (e.g. Ferrer and Malabarba 2013; Costa et al. 2020a, c; Vilaro et al. 2020). In southern Brazil, the most species-rich trichomycterine genus is *Cambeva* Katz, Barbosa, Mattos & Costa, 2018, presently with 27 valid species (see below), among which only four were described before 1992 (Katz et al. 2018). The number of known species of *Cambeva* has been quickly increased in recent years as a result of field inventories in previously under-sampled areas and the increasingly interest in trichomycterid taxonomy after Costa (1992) and de Pinna (1992), but some areas remain unsampled. Species of *Cambeva* are present in both large river basins such as the Paraná, São Francisco and Uruguai basins, and in small coastal river drainages. The greatest concentration of species occurs in the Rio Paraná basin, with a total of 16 species (Katz and Costa 2020), including *C. papillifera* (Wosiacki & Garavello, 2005), new combination, which exhibits the typical combination of external morphological features of *Cambeva* (i.e. pectoral fin lacking a filament at the tip of the first ray and hypertrophied cheek muscles), but equivocally omitted in Katz et al. (2018). Among the species not occurring in the Rio Paraná basin, two occur in the São Francisco basin (Costa 1992), five in the Lagoa dos Patos system (Ferrer and Malabarba 2011, 2013), two in the Rio Uruguai basin (Datovo et al. 2012; Costa et al. 2020d), and three in the Rio Ribeira de Iguape and smaller coastal basins (Eigenmann 1918; Bizerril 1994; Wosiacki and Oyakawa 2005). However, no species was described from the wide area, about 250 km long, between the coastal river basins of northern Santa Catarina state (Bizerril 1994; Katz and Barbosa 2014) and the southern end of the Atlantic Forest, in the Lagoa dos Patos system.

In the past two decades, the river basins of the southern portion of the Atlantic Forest have been inventoried by members of the Laboratory of Systematics and Evolution of Teleost Fishes team (UFRJ), and more recently exhaustively sampled by one of us (CRM), revealing a great species diversity comparable to those already recorded for neighbouring areas. The objective of this paper is to provide formal descriptions for two of the new species collected in this area.

Material and methods

Morphometric and meristic data were taken following Costa (1992), with modifications proposed by Costa et al. (2020a); measurements are presented as percent of standard length (SL), except for those related to head morphology, which are expressed as percent of head length. Fin-ray counts include all elements; vertebra counts include all vertebrae except those participating in the Weberian apparatus; the compound caudal centrum was counted as a single element; counts of vertebrae and procurrent fin rays were made only in cleared and stained specimens; counts of principal-fin rays were made in all available specimens, except juveniles about 30 mm SL or

less; counts of jaw teeth were approximate, due to their irregular arrangement, great number and frequent loss, making impossible accurate counts. Specimens were cleared and stained for bone and cartilage (C&S in lists of specimens) following Taylor and Van Dyke (1985). Osteological characters included in descriptions are those belonging to structures with informative variability for diagnosing species of *Cambeva*, including the mesethmoidal region, suspensorium and opercular apparatus, and hyoid skeleton. Terminology for bones followed Bockmann et al. (2004), except for ‘tendon-bone supraorbital’, here called ‘sesamoid supraorbital’ following Adriaens et al. (2010); ‘urohyal’, here called ‘parurohyal’ following Arratia and Schultze (1990); and ‘pleural rib’, here called simply ‘rib’ following the morphological study by Britz and Bartsch (2003) supporting to exist a single rib type in teleosts. Osteological illustrations were made using a stereomicroscope Zeiss Stemi SV 6 with camera lucida. Cephalic laterosensory system terminology follows Arratia and Huaquin (1995), with modifications proposed by Bockmann et al. (2004). Specimens are deposited in the ichthyological collection of the Institute of Biology of the Federal University of Rio de Janeiro, Rio de Janeiro city and in the Centre of Agrarian and Environmental Sciences, Federal University of Maranhão, Campus Chapadinha (CICCAA). Comparative material is listed in Costa et al. (2020a). Throughout the text, geographical names follow Portuguese terms used in the region, thus avoiding common errors or generalizations when tentatively translating them to English, besides making easier their identification in the field.

Results

Cambeva barbosae sp. nov.

<http://zoobank.org/A0C5B36A-9A31-4075-B5A1-A3D9C6548105>

Figs 1, 2, 3A–E, 4A–C, Table 1

Holotype. UFRJ 10000, 67.6 mm SL; Brazil: Santa Catarina state: Águas Mornas municipality: Rio Cubatão do Sul basin, 27°39'51"S, 48°51'26"W, about 130 m asl; A.M. Katz, F.R. Pereira & M.A. Barbosa, 31 May 2013.

Paratypes. All from Brazil: Santa Catarina state. Rio Cubatão do Sul: UFRJ 9503, 10, 44.1–71.6 mm SL; UFRJ 9848, 5, 34.1–41.7 mm SL (C&S); collected with holotype. Rio Maruim basin: – UFRJ 9505, 13.3–73.1 mm SL; 27°40'39"S, 48°50'53"W, about 90 m asl; same collectors and date as holotype. – UFRJ 12629, 6, 38.7–62.0 mm SL; stream tributary to Rio Forquilhas, Colônia Santana, São José municipality, 27°32'44"S, 48°42'21"W, about 40 m asl; C.R.M. Feltrin, 15 Nov. 2019. – UFRJ 6924, 10, 31.9–57.6 mm SL; small stream tributary to upper Rio Forquilhas, village of Alto Forquilhas, São José municipality, 27°32'44"S, 48°42'21"W, about 40 m asl; C.R.M. Feltrin, 17 Jun. 2020. Rio Cubatão do Sul basin: UFRJ 6925, 25, 24.8–62.1 mm SL; unnamed stream,



Figure 1. *Cambeva barbosa* sp. nov., UFRJ 10000, holotype, 67.6 mm SL: **A.** left lateral view; **B.** dorsal view; **C.** ventral view.

Águas Mornas municipality, 27°43'16"S, 48°53'23"W, about 190 m asl; C.R.M. Feltrin, 13 Jun. 2020. Rio Biguaçu basin, Biguaçu municipality: UFRJ 11717, 11, 31.6–67.9 mm SL; UFRJ 6921, 3 (C&S), 51.1–58.9 mm SL; Cachoeira Graciosa, 27°26'37"S, 48°40'59"W, about 60 m asl; C.R.M. Feltrin, Aug. 2017. – UFRJ 11872, 2, 54.1–54.9 mm SL; same locality and collector as UFRJ 11717, 27 Nov. 2018. – CICC AA 02617, 2, 53.5–62.3 mm SL; Riacho Canudos, 27°24'30"S, 48°45'17"W, about 70 m asl; C.R.M. Feltrin, 4 Dec. 2017.

Additional material (non-types). Rio Biguaçu basin, Biguaçu municipality: UFRJ 12383, 4; UFRJ 12385, 11; Riacho Canudos, 27°25'20"S, 48°45'13"W, about 30 m asl; B. Mesquita & P.F. Amorim, 16 Aug. 2019. Florianópolis municipality: UFRJ 10603, 10; UFRJ 10669, 2 (C&S); Córrego Grande, Ilha de Santa Catarina, 27°36'10"S, 48°30'12"W, about 15 m asl; A.M. Katz, F. Pereira & P.F. Amorim, 11 Jun. 2015.

Diagnosis. *Cambeva barbosa* differs from all congeners, except *C. castroi* (de Pinna, 1992), *C. concolor* (Costa, 1992), *C. crassicaudata* (Wosiacki & de Pinna 2008), *C. diabola* (Bockmann, Casatti & de Pinna, 2004),

C. guaraquessaba (Wosiacki, 2005), *C. igobi* (Wosiacki & de Pinna, 2008), *C. iheringi* (Eigenmann, 1917), *C. tupinamba* (Wosiacki & Oyakawa, 2005), *C. variegata* (Costa, 1992), *C. ytororo* Terán, Ferrer, Benitez, Alonso, Aguilera & Mirande, 2017, and *C. zonata* (Eigenmann, 1918) by having eight pectoral-fin rays (vs. five to seven in all other species). *Cambeva barbosa* differs from all these species by the following combination of diagnostic features: nine principal dorsal-fin rays (vs. 12–13 in *C. concolor*, *C. iheringi* and *C. variegata*); 19–23 dorsal procurrent caudal-fin rays (vs. 15–16 in *C. guaraquessaba* and *C. tupinamba*; 24–29 in *C. crassicaudata* and *C. igobi*; and 31–35 in *C. ytororo*); 8–12 ventral procurrent caudal-fin rays (vs. 17–19 in *C. crassicaudata*); 36–38 vertebrae (vs. 34–35 in *C. concolor*, *C. iheringi* and *C. variegata*); all jaw teeth incisiform (vs. conical in *C. castroi* and *C. diabola*, anterior teeth sub-incisiform, posterior teeth conical in *C. zonata*); and absence of a dark grey to black bar on the posterior portion of the caudal fin, contrasting with a white to pale yellow zone on the anterior portion of the fin (vs. presence in *C. castroi* and *C. diabola*). Also distinguished from *C. concolor*, *C. crassicaudata*, *C. igobi*, and *C. variegata* by having a distinctive process on the dorsal margin of the quadrate,

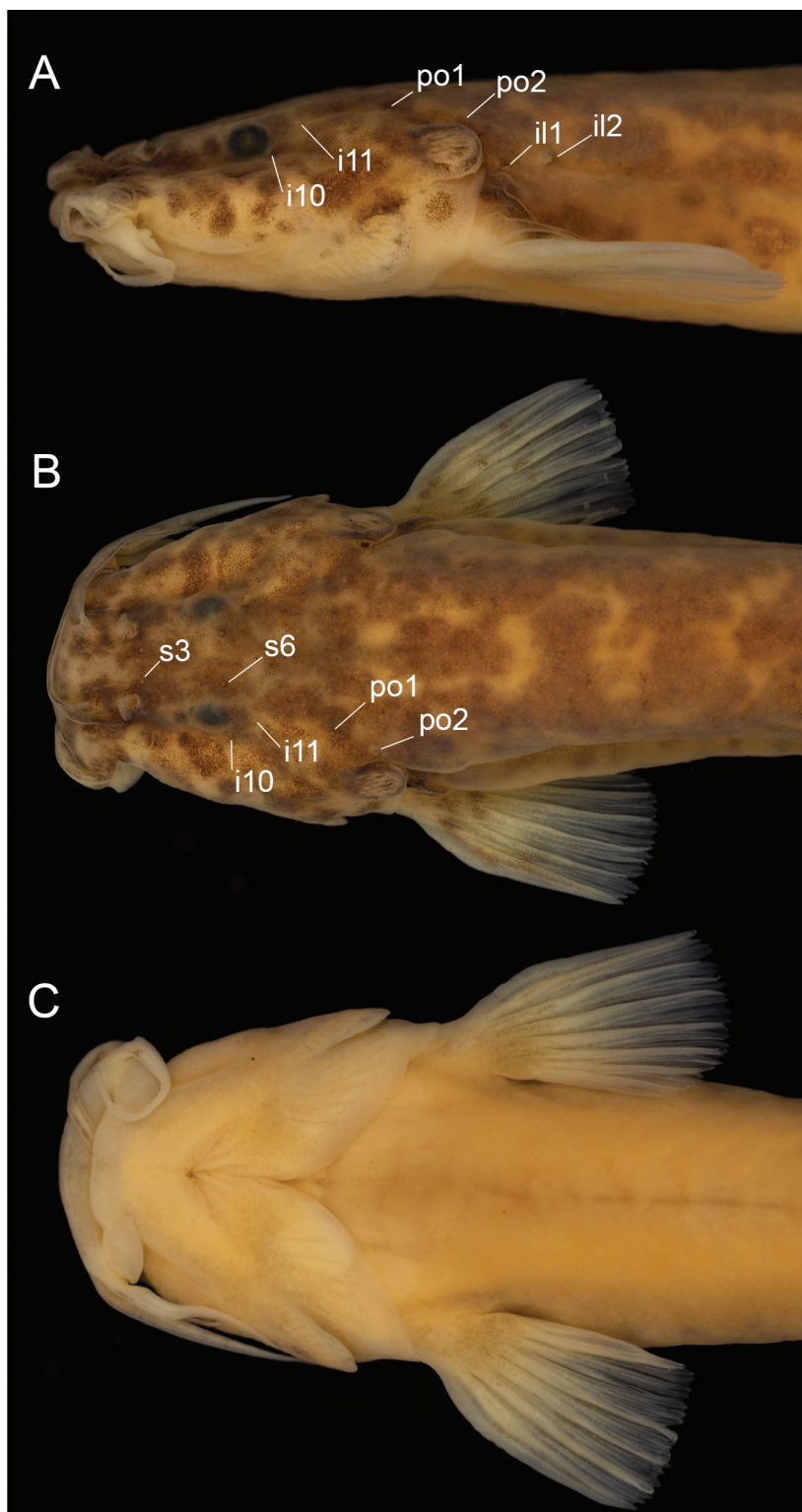


Figure 2. Head of *Cambeva barbosa* sp. nov., UFRJ 10000, holotype, 67.6 mm SL: **A**, left lateral view **B**, dorsal view; **C**, ventral view. Pores of the cephalic latero-sensory system are indicated in **A** and **B**.

just posterior to the cartilage block joining quadrate and metapterygoid (Fig. 4B; vs. absence), and from *C. castroi*, *C. concolor*, *C. crassicaudata*, *C. diabola*, *C. igobi*, *C. variegata* (Costa, 1992), and *C. zonata* by the presence of a distinctive, anteriorly directed process on the lateral margin of the lateral ethmoid (Fig. 4A; vs. absence) and a deep notch between the lateral shell on the opercular

articular facet for the hyomandibula and the opercular articular facet for the preopercle in larger specimens (above about 50 mm SL, Fig. 4B; vs. absence).

Description. Morphometric data appear in Table 1. Body moderately slender, subcylindrical and slightly depressed anteriorly, compressed posteriorly. Greatest

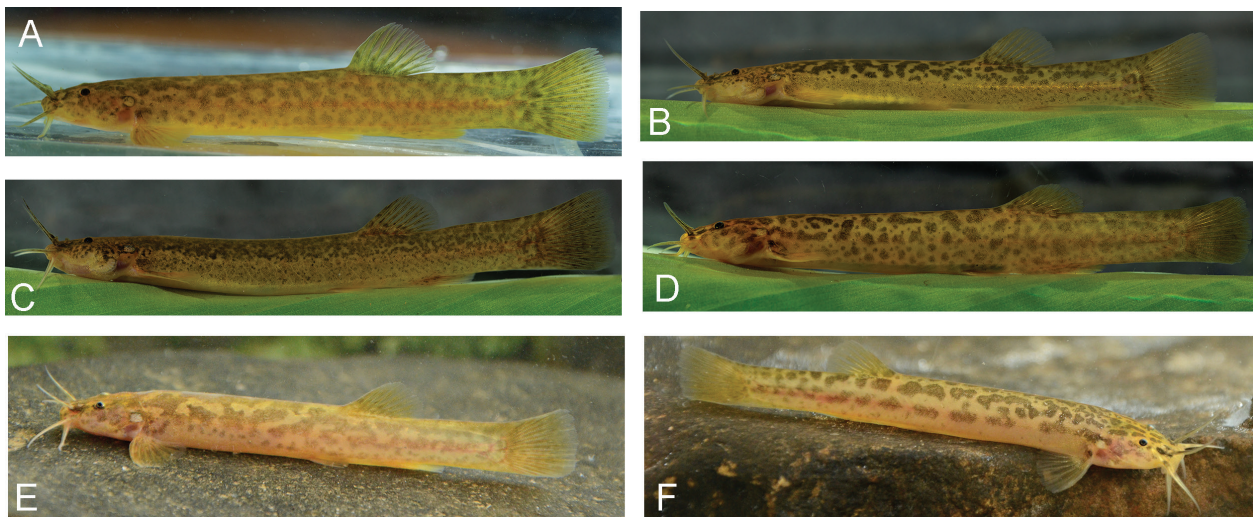


Figure 3. Live specimens (not preserved) of: **A–E.** *Cambeva barbosa* sp. nov.: **A.** From the type locality; **B–D.** From Córrego Grande, Ilha de Santa Catarina; **E.** From Rio Biguaçu basin; **F.** *Cambeva botuvera* sp. nov., from the type locality.

Table 1. Morphometric data of *Cambeva barbosa* sp. nov.

	Holotype	Paratypes (n = 12)
Standard length (mm)	67.6	44.3–71.6
Percent of standard length		
Body depth	14.0	13.9–18.7
Caudal peduncle depth	12.0	11.3–13.0
Body width	10.2	10.2–14.1
Caudal peduncle width	3.1	2.9–4.7
Pre-dorsal length	60.2	61.5–66.6
Pre-pelvic length	54.5	54.9–61.6
Dorsal-fin base length	11.7	10.8–13.8
Anal-fin base length	7.7	7.7–9.1
Caudal-fin length	17.3	14.4–18.5
Pectoral-fin length	14.9	12.1–15.1
Pelvic-fin length	10.3	8.7–11.2
Head length	20.4	19.7–22.8
Percent of head length		
Head depth	45.4	46.6–54.4
Head width	81.3	79.0–89.9
Snout length	40.1	41.2–45.5
Interorbital length	20.7	20.5–25.9
Preorbital length	15.3	13.6–16.7
Eye diameter	12.8	10.8–13.8

body depth in area just anterior to pelvic-fin base. Dorsal profile of head and trunk slightly convex, approximately straight on caudal peduncle; ventral profile straight to slightly convex between lower jaw and end of anal-fin base, straight on caudal peduncle. Skin papillae minute. Anus and urogenital papilla in vertical through anterior portion of dorsal-fin base. Head trapezoidal in dorsal view. Anterior profile of snout convex in dorsal view. Eye small, dorsally positioned in head. Posterior nostril located nearer anterior nostril than orbital rim. Tip of maxillary and rictal barbels reaching posterior half of interopercular patch of odontodes; tip of nasal barbel surpassing posterior margin of orbit, reaching transverse line through middle of interopercular patch of odontodes. Mouth subterminal. Jaw teeth incisiform and slightly curved, 40–52 in premaxilla, 42–45 in dentary, arranged in three or four irregular rows. Branchial

membrane attached to isthmus only at its anterior point. Branchiostegal rays 8 or 9.

Dorsal and anal fins subtriangular; total dorsal-fin rays 11 (ii + II + 7), total anal-fin rays 9 (ii + II + 5); anal-fin origin in vertical through posterior portion of dorsal-fin base, approximately at base of 5th branched dorsal-fin ray. Dorsal-fin origin in vertical between centrum of 19th and 20th vertebrae; anal-fin origin in vertical between centrum of 23rd and 24th vertebra. Pectoral fin subtriangular in dorsal view, posterior margin slightly convex, tip of first pectoral-fin ray not forming filament; total pectoral-fin rays 8 (I + 7). Pelvic fin subtruncate, its extremity in vertical through anterior portion of dorsal-fin base; pelvic-fin bases medially in close proximity; total pelvic-fin rays 5 (I + 4). Caudal fin truncate, postero-dorsal and postero-ventral extremities rounded; total principal caudal-fin rays 13 (I + 11 + I), total dorsal procurent rays 19–23 (xviii–xxii + I), total ventral procurent rays 10–12 (ix–xi + I). Vertebrae 36–38. Ribs 12–13. Two dorsal hypural plates, corresponding to hypurals 4 + 5 and 3, respectively; single ventral hypural plate corresponding to hypurals 1 and 2 and parhypural.

Laterosensory system (Fig. 2A–B). Supraorbital sensory canal continuous, connected to posterior section of infraorbital canal posteriorly. Supraorbital sensory canal with 3 pores: s1, adjacent to medial margin of anterior nostril; s3, adjacent and just posterior to medial margin of posterior nostril; and s6, in transverse line through posterior half of orbit; pore s6 nearer orbit than its paired homologous pore. Anterior segment of infraorbital sensory canal absent; posterior segment with two pores, pore i10, adjacent to ventral margin of orbit, and pore i11, posterior to orbit. Postorbital canal with 2 pores: po1, in vertical line above posterior portion of interopercular patch of odontodes, and po2, in vertical line above posterior portion of opercular patch of odontodes. Lateral line of body short, with 2 pores, posterior-most pore in vertical just posterior to pectoral-fin base.

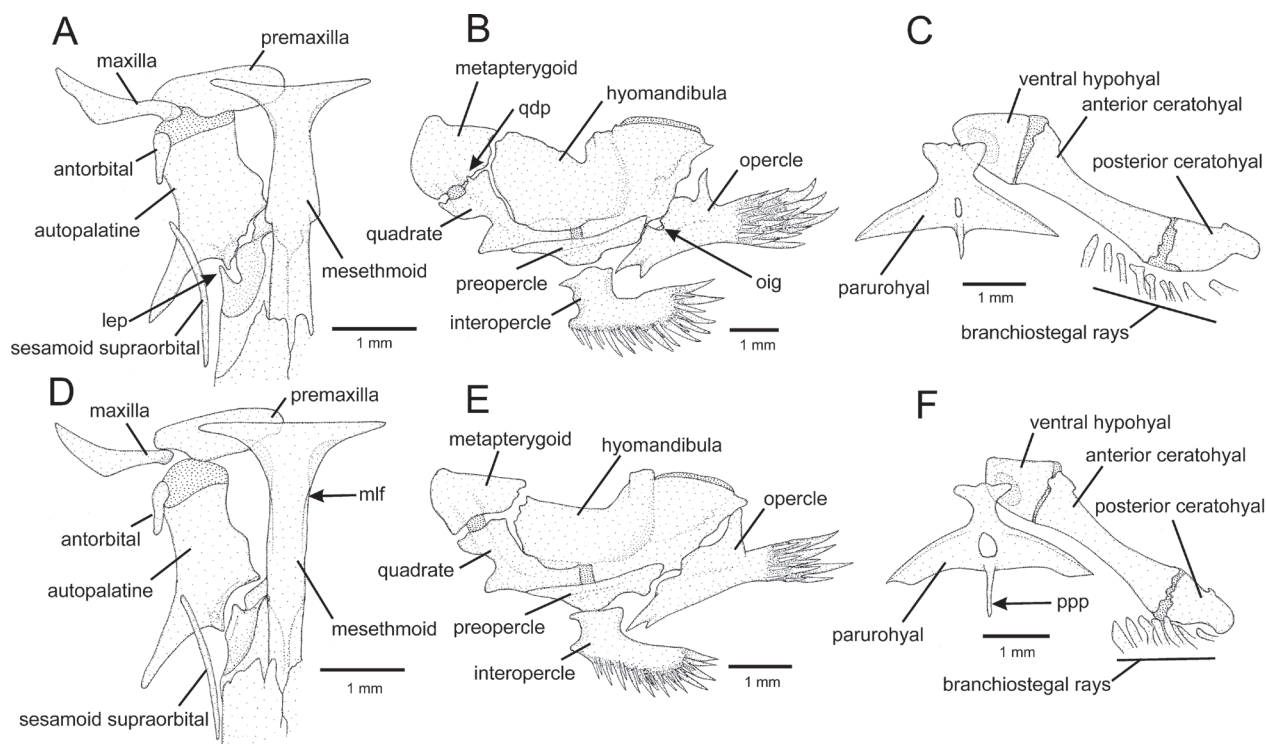


Figure 4. Osteological structures of: **A–C.** *Cambeva barbosa* sp. nov.; **D–F.** *Cambeva botuvera* sp. nov.: **A, D.** Mesethmoidal region and adjacent structures, left and middle portions, dorsal view; **B, E.** Left suspensorium and opercular series, lateral view; **C, F.** Hyoid arch, ventral view. Abbreviations of structures indicated by arrows are: lep, lateral ethmoid lateral process; mlf, mesethmoidal lateral flap; oig, opercular interarticular gap; ppp parurohyal posterior process. Larger stippling represents cartilaginous areas.

Mesethmoidal region (Fig. 4A). Mesethmoid robust, its anterior margin slightly concave; mesethmoid cornu narrow, extremity rounded. Lateral ethmoid connected to autopalatine by weak articular facet, which in specimens larger than about 50 mm SL is latero-posteriorly edged by deep notch posteriorly followed by prominent anteriorly directed process. Antorbital thin, drop-shaped; sesamoid supraorbital slender, without processes, its length about three times antorbital length. Premaxilla sub-rectangular in dorsal view, laterally narrowing, moderate in length, slightly longer than maxilla. Maxilla boomerang-shaped, slender, slightly curved. Autopalatine sub-rectangular in dorsal view, medial margin sinuous, lateral margin slightly concave; autopalatine posterolateral process well-developed, narrow, its length about two thirds autopalatine length excluding posterolateral.

Cheek region (Fig. 4B). Metapterygoid thin, subtriangular, large, its largest length about equal horizontal length of quadrate excluding dorsal process. Quadrate slender, dorsal process with constricted base, dorsoposterior margin separated from hyomandibula outgrowth by small interspace; small process on dorsal margin, just posterior to cartilage block joining quadrate and metapterygoid, laterally overlapping ventral part of metapterygoid. Hyomandibula long, with well-developed anterior outgrowth; middle portion of dorsal margin of hyomandibula outgrowth with shallow concavity. Opercle relatively robust, opercular odontode patch depth about four fifths of dorsal hyomandibula articular facet, with 15–18 odontodes;

odontodes pointed, slightly curved, arranged in irregular transverse rows; dorsal process of opercle short and pointed; opercular articular face for hyomandibula with prominent trapezoidal lateral flap, separated from small articular facet for preopercle by deep gap. Interopercle moderate, about two thirds hyomandibula length, with 30–36 odontodes; odontodes pointed, arranged in irregular longitudinal rows. Preopercle compact, with short ventral flap.

Hyoid region (Fig. 4C). Parurohyal robust, lateral process triangular, straight, laterally directed, tip pointed; parurohyal head well-developed, with indistinct antero-lateral paired process; middle foramen small and elliptical; posterior process short, about two thirds distance between anterior margin of parurohyal and anterior insertion of lateral process. Ceratohyals slender.

Colouration in alcohol (Fig. 1). Flank, dorsum and head side light brown. Dorsum, flank and head with pale dark brown spots, variable in size and shape, often inconspicuous in specimens from Rio Biguaçu basin. Venter yellowish grey. Darker pigment concentrated between anterior and posterior nostrils, around opercular patch of odontodes and posterior portion of caudal peduncle; nasal and maxillary barbels dark brown, rictal barbel pale brown with dark brown base. Ventral surface of head yellowish white. Unpaired fins dark yellowish grey, dark brown spots on basal portion of dorsal and caudal fins. Paired fins pale yellow, basal portion of pectoral fin dark yellowish grey.

Colouration in life (Figs. 2A–E). Similar to colouration in alcohol, but yellow pigmentation more intense on trunk and fins orangish yellow in unspotted specimens from Rio Biguaçu basin.

Distribution and habitat. *Cambeva barbosa* occurs in fast-flowing low-altitude streams (about 15–190 m asl), of coastal river basins, between the Biguaçu and the Cubatão do Sul river basins, as well as in smaller drainages in the Santa Catarina island (Fig. 5).

Etymology. *Cambeva barbosa* is named in honour of the Brazilian ichthyologist Maria Anais Barbosa, for her efforts to collect and study trichomycterines from Santa Catarina.

Remarks. The species collected in the Santa Catarina island and identified as *Trichomycterus* sp. by Bertaco (2009), probably is *Cambeva barbosa*, since both were collected at the same locality in Córrego Grande.

Cambeva botuvera sp. nov.

<http://zoobank.org/145BAE1A-008B-4D80-BDFD-C814347B73DB>

Figs 3F, 4D–F, 6, 7, Table 1

Holotype. UFRJ 6911, 66.9 mm SL; Brazil: Santa Catarina state: Botuverá municipality: village of Ourinhos: Ribeirão Ourinhos, Rio Itajaí-Mirim basin, 27°14'22"S, 49°10'22"W, about 160 m asl; C.R.M. Feltrin, 9 Apr. 2018.

Paratypes. All from Brazil: Santa Catarina state: de Botuverá municipality: Rio Itajaí-Mirim basin. UFRJ 11920, 6, 36.4–70.9 mm SL; collected with holotype. – UFRJ 12196, 14, 42.6–80.0 mm SL; UFRJ 6912, 3, 39.2–57.3 mm SL (C&S); stream belonging to the Rio Ourinhos subdrainage, Ourinhos, 27°14'22"S, 49°10'22"W, about 160 m asl; C.R.M. Feltrin, 26 Aug. 2018. – UFRJ 12200, 8, 29.9–72.5 mm SL; stream belonging to the Rio Ourinhos subdrainage, Ourinhos, 27°14'6"S, 49°10'10"W, about 170 m asl; C.R.M. Feltrin, 26 Aug. 2018. – CIC-CAA 12618, 5, 48.1–66.4 mm SL; stream belonging to the Rio Ourinhos subdrainage, Ourinhos, 27°14'34"S, 49°10'39"W, about 170 m asl; C.R.M. Feltrin, 23 Oct. 2018. – UFRJ 12202, 9, 43.3–71.6 mm SL; stream tributary of Rio Itajaí-Mirim, 27°12'18"S, 49°8'14"W, about 170 m asl; C.R.M. Feltrin, 24 Oct. 2018. – UFRJ 11918, 15, 31.4–81.1 mm SL; stream tributary of Rio Itajaí-Mirim near Lajeado Baixo, 27°12'18"S, 49°8'14"W, about 170 m asl; C.R.M. Feltrin, 8 Apr. 2018. – UFRJ 12195, 7, 31.0–40.0 mm SL; UFRJ 12201, 9, 32.8–64.4 mm SL; stream tributary of Rio Itajaí-Mirim near Lajeado Baixo, 27°12'18"S, 49°8'14"W, about 170 m asl; C.R.M. Feltrin, 25 Aug. 2018.

Diagnosis. *Cambeva botuvera* is distinguished from all other species of the genus, except *C. balios* (Ferrer & Malabarba, 2013), *C. cubataonis* (Bizerril, 1994),

C. davis (Haseman, 1911), *C. diatropoporos* (Ferrer & Malabarba, 2013), *C. guareiensis* Katz & Costa, 2020, *C. horacioi* Reis, Frota, Fabrin & da Graça, 2020, *C. papillifera*, *C. perkos* (Datovo, Carvalho & Ferrer, 2012), *C. plumbea* (Wosiacki, 2005), *C. stawiarski* (Miranda Ribeiro, 1968), and *C. tropeira* (Ferrer & Malabarba, 2011), by having seven pectoral-fin rays (vs. five, six or eight). *Cambeva botuvera* differs from these congeners by the following combination of character states: 16–20 dorsal procurrent caudal-fin rays (vs. 14–15 in *C. tropeira*, 21–22 in *C. cubataonis* and *C. plumbea*, and 27–29 in *C. stawiarski*); 14–16 ventral procurrent caudal-fin rays (vs. 9–13 in *C. balios*, *C. cubataonis*, *C. davis*, *C. diatropoporos*, and *C. guareiensis*); 39–40 vertebrae (vs. 35–38 in *C. cubataonis*, *C. diatropoporos*, *C. guareiensis*, *C. horacioi*, and *C. stawiarski*); eight or nine branchiostegal rays (vs. ten in *C. perkos* and *C. stawiarski*); jaw teeth conical (incisiform in *C. davis*, *C. guareiensis* and *C. stawiarski*); minute papillae on the ventral surface of the head (vs. hypertrophied in *C. papillifera*); relatively long maxillary and rictal barbels, reaching between the interopercular patch of odontodes and the pectoral-fin base (vs. rudimentary in *C. papillifera*); pelvic fin and girdle well-developed (vs. absent in *C. tropeira*); anterior segment of the latero-sensory infraorbital series absent (vs. present in *C. diatropoporos* and *C. tropeira*); and colouration consisting of dorsum and dorsal portion of flank with rounded brown blotches, without a distinctive yellow longitudinal zone on the dorsal portion of the flank (vs. minutes dots or no distinctive marks in *C. papillifera* and *C. plumbea*; presence of a distinctive yellow longitudinal zone on the dorsal portion of the flank in *C. perkos*). *Cambeva botuvera* is also distinguished from *C. balios*, *C. cubataonis*, *C. davis*, *C. diatropoporos*, *C. guareiensis*, *C. plumbea*, and *C. tropeira* by having a long posterior process of the parurohyal, slightly longer than the length between the anterior-most point of parurohyal head and lateral process insertion (Fig. 4F; vs. shorter).

Description. Morphometric data appear in Table 2. Body moderately slender, subcylindrical and slightly depressed anteriorly, compressed posteriorly. Greatest body depth in area just anterior to pelvic-fin base. Dorsal profile of head and trunk slightly convex, approximately straight on caudal peduncle; ventral profile straight to slightly convex between lower jaw and end of anal-fin base, straight on caudal peduncle. Skin papillae minute. Anus and urogenital papilla in vertical through anterior portion of dorsal-fin base. Head trapezoidal in dorsal view. Anterior profile of snout convex in dorsal view. Eye small, dorsally positioned in head. Posterior nostril located nearer anterior nostril than orbital rim. Tip of maxillary and rictal barbels reaching area between interopercular patch of odontodes and pectoral-fin base; tip of nasal barbel reaching area between eye and opercular patch of odontodes. Mouth subterminal. Jaw teeth 40–42 in both premaxilla

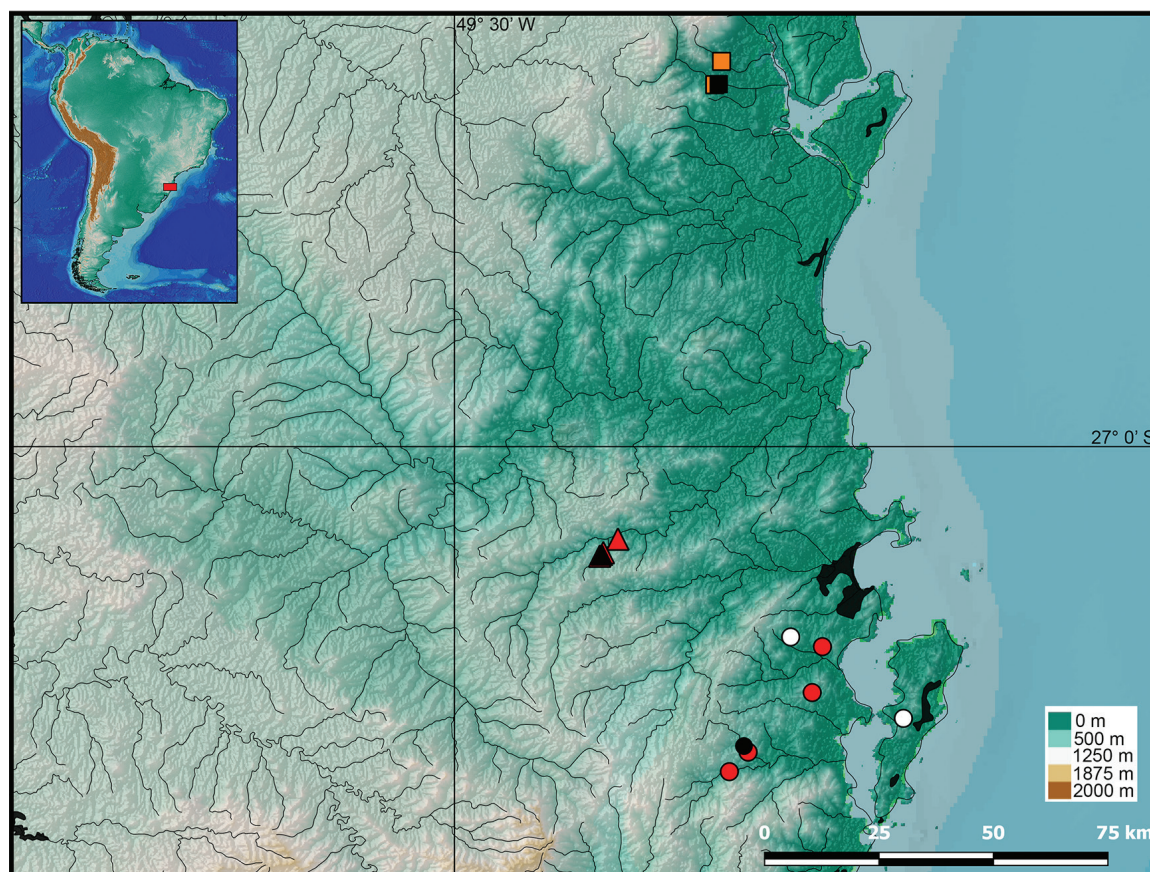


Figure 5. Map of geographical distribution of *Cambeva* in isolated coastal basins in the southern end of the Atlantic Forest, southern Brazil: *C. barbosa* sp. nov. (dots), *C. botuvera* sp. nov. (triangles), *C. cubataonis* (squares); black symbols are type localities, red symbols are paratypes of the new species, and white symbols are additional material, non-types.

Table 2. Morphometric data of *Cambeva botuvera* sp. nov.

	Holotype	Paratypes (n = 12)
Standard length (mm)	66.9	39.2–81.1
Percent of standard length		
Body depth	14.7	13.2–17.9
Caudal peduncle depth	11.6	10.1–12.6
Body width	9.5	9.1–12.7
Caudal peduncle width	3.2	2.8–4.5
Pre-dorsal length	62.2	61.0–66.8
Pre-pelvic length	57.6	55.1–61.3
Dorsal-fin base length	12.5	10.1–11.9
Anal-fin base length	9.9	8.5–10.9
Caudal-fin length	15.8	13.7–17.4
Pectoral-fin length	13.1	11.7–13.8
Pelvic-fin length	8.4	7.9–10.1
Head length	20.9	19.1–21.8
Percent of head length		
Head depth	46.9	44.7–50.8
Head width	80.7	77.1–85.0
Snout length	42.3	41.9–44.7
Interorbital length	22.0	21.4–25.0
Preorbital length	14.4	14.2–15.8
Eye diameter	9.7	9.7–13.2

and dentary, irregularly arranged, pointed and slightly curved. Branchial membrane attached to isthmus only at its anterior point. Branchiostegal rays 8 or 9.

Dorsal and anal fins subtriangular; total dorsal-fin rays 12 (iii + II + 7), total anal-fin rays 9 (ii + II + 5);

anal-fin origin in vertical through middle of dorsal-fin base or slightly posterior to it, approximately at base of 5th branched dorsal-fin ray. Dorsal-fin origin in vertical through centrum of 21st or 22nd vertebra; anal-fin origin in vertical through centrum of 25th vertebra. Pectoral fin subtriangular in dorsal view, posterior margin slightly convex, first pectoral-fin ray not terminating in filament; total pectoral-fin rays 7 (I + 6). Pelvic fin subtruncate, its extremity in vertical through anterior portion of dorsal-fin base; pelvic-fin bases medially in close proximity; total pelvic-fin rays 5 (I + 4). Caudal fin truncate, postero-dorsal and postero-ventral extremities rounded; total principal caudal-fin rays 13 (I + 11 + I), total dorsal procurent rays 16–19 (xv–xix + I), total ventral procurent rays 12–16 (xi–xv + I). Vertebrae 39–40. Ribs 12 or 13. Two dorsal hypural plates, corresponding to hypurals 4 + 5 and 3, respectively, often coalesced to form single plate; single ventral hypural plate corresponding to hypurals 1 and 2 and parhypural.

Laterosensory system (Fig. 7A, B). Supraorbital sensory canal continuous, connected to posterior section of infraorbital canal posteriorly. Supraorbital sensory canal with 3 pores: s1, adjacent to medial margin of anterior nostril; s3, adjacent and just posterior to medial margin of posterior nostril; and s6, in transverse line through posterior half of orbit; pore s6 nearer orbit than its paired



Figure 6. *Cambeva botuvera* sp. nov., UFRJ 6911, holotype, 66.9 mm SL: **A.** left lateral view; **B.** dorsal view; **C.** ventral view.

homologous pore. Single infraorbital sensory canal segment, with two pores, corresponding to pore i10, adjacent to ventral margin of orbit, and pore i11, posterior to orbit; anterior segment of infraorbital canal absent. Postorbital canal with 2 pores: po1, in vertical line above posterior portion of interopercular patch of odontodes, and po2, in vertical line above posterior portion of opercular patch of odontodes. Lateral line of body short, with 2 pores, posterior-most pore in vertical just posterior to pectoral-fin base.

Mesethmoidal region (Fig. 4D). Mesethmoid robust, its anterior margin slightly concave; mesethmoid cornu narrow, extremity rounded; narrow lateral flap on intersection between cornu and main bone axis, posteriorly extending parallel to lateral bone margin. Lateral ethmoid connected to autopalatine by weak articular facet; minute lateral projection on lateral ethmoid margin close to middle portion of sesamoid supraorbital, often absent. Antorbital thin, drop-shaped; sesamoid supraorbital slender, without processes, its length about three times antorbital length. Pre-maxilla sub-trapezoidal in dorsal view, laterally narrowing, moderate in length, slightly longer than maxilla. Maxilla boomerang-shaped, slender, slightly curved. Autopalatine sub-rectangular in dorsal view, medial margin sinuous, lateral margin slightly concave; autopalatine posterolateral

process well-developed, narrow, its length about two thirds autopalatine length excluding posterolateral.

Cheek region (Fig. 4E). Metapterygoid thin, sub-triangular, large, its largest length slightly shorter than horizontal length of quadrate excluding dorsal process. Quadrate slender, dorsal process with constricted base, dorsoposterior margin separated from hyomandibula outgrowth by small interspace. Hyomandibula long, with well-developed anterior outgrowth; middle portion of dorsal margin of hyomandibula slightly concave. Opercle relatively slender, opercular odontode patch depth about half length of dorsal hyomandibula articular facet, with 15–18 odontodes; odontodes pointed, nearly straight, arranged in irregular transverse rows; dorsal process of opercle short and pointed; opercular articular faces for hyomandibula and preopercle rounded and in close proximity. Interopercle moderate, about two thirds hyomandibula length, with 25–30 odontodes; odontodes pointed, arranged in irregular longitudinal rows. Preopercle compact, with short ventral flap.

Hyoid region (Fig. 4F). Parurohyal robust, lateral process sub-triangular, slightly curved, latero-posteriorly directed, tip pointed; parurohyal head well-developed, with indistinct anterolateral paired process; middle foramen broad, oval; posterior process long,

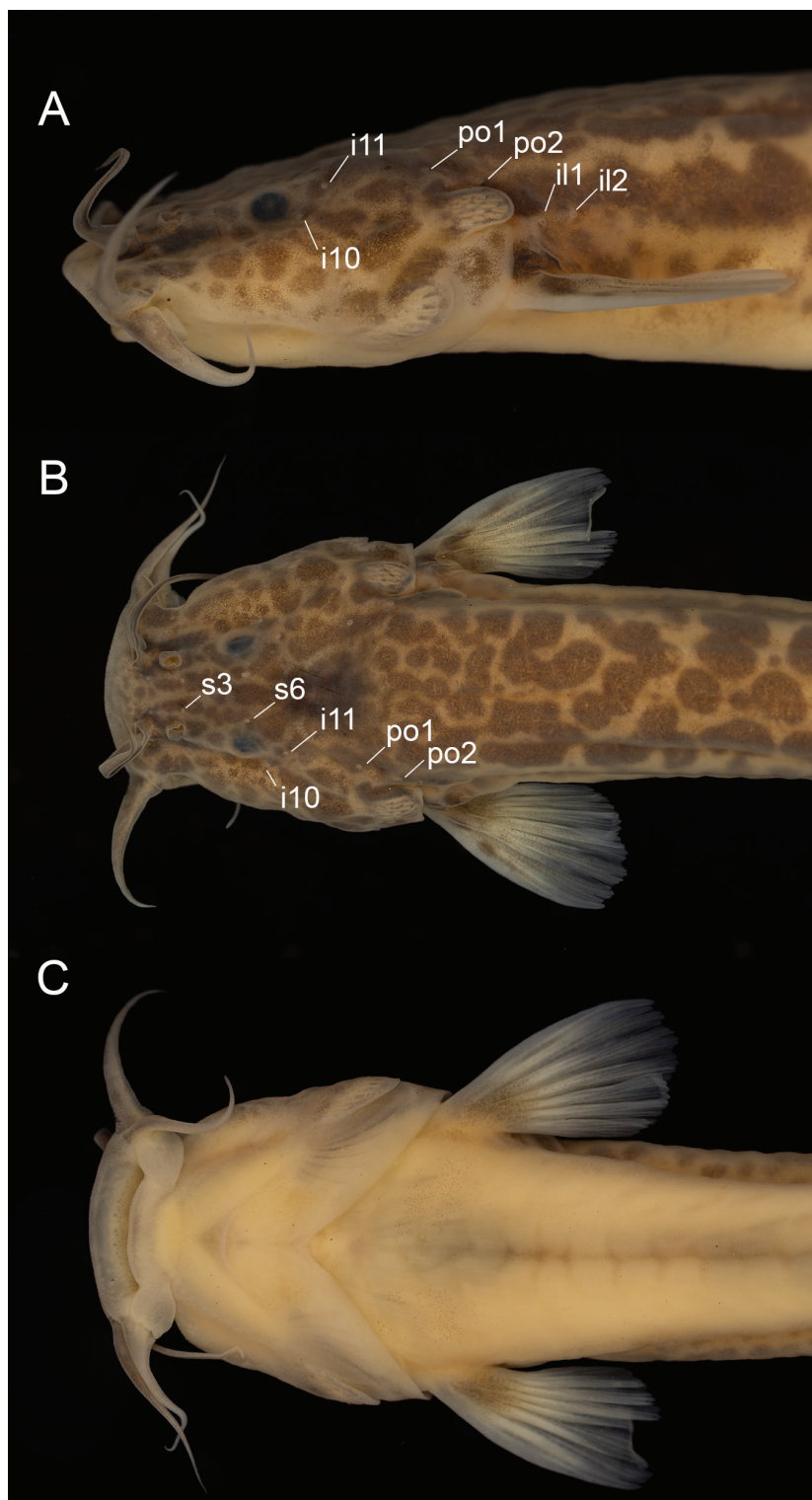


Figure 7. Head of *Cambeva botuvera* sp. nov., UFRJ 6911, holotype, 66.9 mm SL: **A.** left lateral view; **B.** dorsal view; **C.** ventral view. Pores of the cephalic latero-sensory system are indicated in A and B.

slightly longer than distance between anterior margin of parurohyal and anterior insertion of lateral process. Ceratohyals slender.

Colouration in alcohol (Fig. 6). Flank, dorsum and head side pale yellowish brown. Dorsum and dorsal portion of flank with rounded brown blotches, darker and often horizontally coalesced along lateral midline, sometimes

forming interrupted or complete darker stripe. Ventral part of flank with pale grey spots, often inconspicuous or absent. Small dark brown spots on lateral and dorsal surfaces of head, darker pigment concentrated between anterior and posterior nostrils and around opercular patch of odontodes; nasal barbel dark brown, maxillary and rictal barbels pale brown with dark brown bases. Venter and ventral surface of

head yellowish white. Unpaired fins hyaline with yellowish brown bases. Pectoral fin hyaline with dark brown spots on basal portion. Pelvic fin whitish hyaline.

Colouration in life (Fig. 3F). Similar to colouration in alcohol, but yellow pigmentation slightly more intense on trunk and fins.

Distribution and habitat. *Cambeva botuvera* occurs in fast-flowing low-altitude streams (about 160–170 m asl), of the Rio Itajai-Mirim basin (Fig. 5).

Etymology. The name *botuvera* is an allusion to the occurrence of the species in the municipality of Botuverá, Santa Catarina, southern Brazil. This name is derived from the Tupi-Guarani, possibly meaning brilliant mountain.

Discussion

Cambeva is a morphologically homogeneous genus, with relatively little external morphological variation when compared to the closely related genus *Trichomycterus* (sensu Katz et al. 2018). However, as here and elsewhere observed (Costa et al. 2020d), osteological characters may be useful to distinguish closely species and to tentatively support relationship hypotheses. Unfortunately, due to the absence of osteological data in descriptions of species that are rare in ichthyological collections, present diagnoses are still directed to combinations of character states of the external morphology that may be checked in original descriptions (see diagnoses above). Anyway, the present osteological comparative analysis indicates some osteological characters potentially diagnosing intrageneric clades that will help to support species allocation in future studies.

Molecular phylogenies including species of *Cambeva* have been directed to more inclusive trichomycterid groups (Ochoa et al. 2017, 2020; Katz et al., 2018; Costa et al., 2020c), consequently comprising a limited sample of taxa belonging to this genus. Therefore, phylogenetic relationships among species of *Cambeva* are still poorly known (Costa et al., 2020d). However, the available molecular analyses, including a recent unilocus analysis (Donin et al. 2020), have corroborated similar intrageneric clades, including a clade named as the *C. balios* group by Costa et al. (2020d), comprising all species from the Lagoa dos Patos system and part of the species from the Paraná-Uruguay system, and another clade, here named as *C. davisii* group, including species from the Rio Paraná basin and smaller coastal basins. Costa et al. (2020d) described some osteological character states presumably supporting the *C. balios* group and a subclade, but no morphological feature supporting the *C. davisii* group or its subclades has been described.

The present comparative analysis suggests that the new species herein described do not belong to a single intrageneric clade. According to Costa et al. (2020d), species of the *C. balios* group have a comparatively long premaxilla,

distinctively longer than the maxilla (Costa et al. 2020d: fig. 2A), although this condition is not so evident in *C. balios* (e.g. Ferrer and Malabarba 2013: fig. 2A). Costa et al. (2020d: fig. 2B) also assigned the presence of a short process on the anteroventral portion of the metapterygoid for a subclade of the *C. balios* group, including at least *C. flavopicta* Costa, Feltrin & Katz, 2020 and *C. poikilos* Ferrer & Malabarba, 2013, but possibly this unique derived character state is also present in other species of the *C. balios* group, since a small projection at the same place is present in *C. balios*. *Cambeva flavopicta* and *C. poikilos* share a series of unique derived features in the mesethmoidal region, including a robust autopalatine with a short postero-lateral process (Costa et al. 2020d: fig. 2A). In the species here described, the premaxilla is not so long, there is no similar process on the metapterygoid, and the autopalatine is relatively slender, with a well-developed postero-lateral process (Fig. 4A, D), as primitively occurring in other trichomycterine taxa.

Bockmann et al (2004: fig. 6) described an osseous contact area reinforcing metapterygoid-quadrate connection as a unique apomorphic condition in *C. diabola*. In fact, although variable in shape and size, a flat small process on the dorsal margin of quadrate, laterally overlapping metapterygoid and situated just posterior to the syncondrial joint between the metapterygoid and the quadrate, is also present in species of the *C. davisii* group, including at least *C. castroi*, *C. davisii*, *C. guareiensis* and *C. zonata*. Among species herein described, this process is small but evident in *C. barbosa* (Fig. 4B), highly suggesting its inclusion in the *C. davisii* group. In *C. botuvera*, the metapterygoid and quadrate are posteriorly separate and there is no process (Fig. 4E). On the other hand, the lateral ethmoid of *C. barbosa* bears a deep notch just posterior to the articular face for the autopalatine, posteriorly followed by a prominent anteriorly directed process (Fig. 4A). A similar condition occurs at least in *C. diatropoporos* and *C. poikilos* (Ferrer and Malabarba 2013: fig. 2B), two species of the *C. balios* group. However, both *C. flavopicta* and species of the *C. davisii* group often have a small notch followed by a minute process at the same position, suggesting that this morphological feature may be a basal condition for a more inclusive clade including both the *C. balios* and *C. davisii* groups.

Phylogenetic relationships of *C. botuvera* are still obscure, since it does not exhibit derived osteological character states here described for species of the *C. davisii* group and those described by Costa et al. (2020d) for the *C. balios* group. However, the presence of a lateral flap on the intersection between the cornu and main axis of the mesethmoid, posteriorly extending parallel to the lateral bone margin (Fig. 4D) suggests that *C. botuvera* may be more closely related to the *C. balios* group, since a similar condition was observed in some species of this group, including *C. balios*, *C. poikilos*, and *C. tropeira*.

Presently, three species are known from the coastal river basins of the Atlantic Forest of southern Brazil, comprising the two new species herein described and *C. cubataonis*

(Bizerril, 1994) (Fig. 5). All these species have similar colour patterns (i.e. dark brown spots over flank, Figs 1, 6; Katz and Barbosa 2014: fig. 1) and distinction is not easy using only characters of the external morphology. However, as occurring in other congeners and most trichomycterines, bone morphology highly differs in these species, showing important diagnostic character states, mainly concentrated in the mesethmoidal region and cheek bones (see discussion above and Fig. 4). Therefore, the regular use of such structures in taxonomical studies will substantially improve trichomycterine taxonomy, especially in groups for which molecular data are not widely available.

Acknowledgements

We are grateful to Alexandre Bianco, Beatriz Mesquita, Caroline Freitas, Filipe Pereira, Georg Beckmann, João de Bittencourt Vitto, José Leonardo Mattos, Luiz Fernando Ugioni, Maria Anaïs Barbosa, Pedro Amorim, and Ronaldo dos Santos Jr, for collecting specimens of the new species or assistance during field expeditions in southern Brazil; and to Morevy Cheffe, Roger Dalcin and Vinícius Abilhoa for sending important comparative material. The final version of the manuscript benefitted from criticisms provided by Walter Azevedo-Santos. Instituto do Meio Ambiente, Santa Catarina, and Instituto Chico Mendes de Conservação da Biodiversidade provided collecting permits. This work was partially supported by Conselho Nacional de Desenvolvimento Científico e Tecnológico (CNPq; grant 307349/2015-2 to WJEMC).

References

- Adriaens D, Baskin JN, Coppens H (2010) Evolutionary morphology of trichomycterid catfishes: About hanging on and digging in. In: Nelson JS, Schultze HP, Wilson MVH (Eds) *Origin and Phylogenetic Interrelationships of Teleosts*. Verlag Dr. Friedrich Pfeil, München, 337–362.
- Abilhoa V, Braga RR, Bornatowski H, Vitule JRS (2011) Fishes of the Atlantic Rain Forest streams: ecological patterns and conservation. In: Grillo O, Venora G (Eds) *Changing Diversity in Changing Environmental*. InTech, Rijeka, 259–282. <https://doi.org/10.5772/24540>
- Arratia G, Huaquin L (1995) Morphology of the lateral line system and of the skin of diplomystid and certain primitive loricarioid catfishes and systematic and ecological considerations. *Bonner Zoologische Monographien* 36: 1–110.
- Arratia G, Schultze H-P (1990) The urohyal: development and homology within Osteichthyan. *Journal of Morphology* 203: 247–282. <https://doi.org/10.15560/5.4.898>
- Bertaco VA (2009) Freshwater fishes, Ilha de Santa Catarina, Brazil. *Check List* 5: 898–902.
- Bizerril CRSF (1994) Descrição de uma nova espécie de *Trichomycterus* (Siluroidei, Trichomycteridae) do Estado de Santa Catarina, com uma sinopse da composição da família Trichomycteridae no leste Brasileiro. *Arquivos de Biologia e Tecnologia* 37: 617–628.
- Bockmann FA, Casatti L, de Pinna MCC (2004) A new species of trichomycterid catfish from the Rio Paranapanema, southeastern Brazil (Teleostei; Siluriformes), with comments on the phylogeny of the family. *Ichthyological Exploration of Freshwaters* 15: 225–242.
- Britz R, Bartsch P (2003) The myth of dorsal ribs in gnathostome vertebrates. *Proceedings of the Royal Society of London, Biological Sciences Series B*, 270 S1–S4. <https://doi.org/10.1098/rsbl.2003.0035>
- Costa WJEM (1992) Description de huit nouvelles espèces du genre *Trichomycterus* (Siluriformes: Trichomycteridae), du Brésil oriental. *Revue française d'Aquariologie et Herpétologie* 18: 101–110.
- Costa WJEM (2009) Peixes Aplocheilóideos da Mata Atlântica Brasileira: História, Diversidade e Conservação/ Aplocheiloid Fishes of the Brazilian Atlantic Forest: History, Diversity and Conservation. Museu Nacional UFRJ, Rio de Janeiro, 172 pp.
- Costa WJEM, Feltrin CRM, Katz AM (2020d) A new species from subtropical Brazil and evidence of multiple pelvic fin losses in catfishes of the genus *Cambeva* (Siluriformes, Trichomycteridae). *Zoosystematics and Evolution* 96: 715–722. <https://doi.org/10.3897/zse.96.56247>
- Costa WJEM, Henschel E, Katz AM (2020b) Multigene phylogeny reveals convergent evolution in small interstitial catfishes from the Amazon and Atlantic forests (Siluriformes: Trichomycteridae). *Zoologica Scripta* 49: 159–173. <https://doi.org/10.1111/zsc.12403>
- Costa WJEM, Katz AM, Mattos JLO, Amorim PF, Mesquita BO, Vilar do PJ, Barbosa MA (2020a) Historical review and redescription of three poorly known species of the catfish genus *Trichomycterus* from south-eastern Brazil (Siluriformes: Trichomycteridae). *Journal of Natural History* 53: 2905–2928. <https://doi.org/10.1080/00222933.2020.1752406>
- Costa WJEM, Mattos JLO, Amorim PF, Vilar do PJ, Katz AM (2020c) Relationships of a new species support multiple origin of melanism in *Trichomycterus* from the Atlantic Forest of south-eastern Brazil (Siluriformes: Trichomycteridae). *Zoologischer Anzeiger* 288: 74–83. <https://doi.org/10.1016/j.jcz.2020.07.004>
- Datovo A, Carvalho M, Ferrer J (2012) A new species of the catfish genus *Trichomycterus* from the La Plata River basin, southern Brazil, with comments on its putative phylogenetic position (Siluriformes: Trichomycteridae). *Zootaxa* 3327: 33–44. <https://doi.org/10.11646/zootaxa.3327.1.3>
- de Pinna MCC (1992) *Trichomycterus castroi*, a new species of trichomycterid catfish from the Rio Iguaçu of Southeastern Brazil (Teleostei, Siluriformes). *Ichthyological Exploration of Freshwaters* 3: 89–95.
- Donin LM, Ferrer J, Carvalho TP (2020) Taxonomical study of *Trichomycterus* (Siluriformes: Trichomycteridae) from the Ribeira de Iguaçu River basin reveals a new species recorded in the early 20th century. *Journal of Fish Biology*. <https://doi.org/10.1111/jfb.14278>
- dos Reis RB, Frota A, Fabrin TMC, da Graça WJ (2019) A new species of *Cambeva* (Siluriformes, Trichomycteridae) from the Rio Ivaí basin, Upper Rio Paraná basin, Paraná State, Brazil. *Journal of Fish Biology* 96: 350–363. <https://doi.org/10.1111/jfb.14204>
- Eigenmann CH (1918) The Pygidiidae, a family of South American catfishes. *Memoirs of the Carnegie Museum* 7: 259–398. <https://doi.org/10.5962/bhl.title.43951>
- Ferrer J, Malabarba LR (2011) A new *Trichomycterus* lacking pelvic fins and pelvic girdle with a very restricted range in Southern Brazil (Siluriformes: Trichomycteridae). *Zootaxa* 2912: 59–67. <https://doi.org/10.11646/zootaxa.2912.1.5>
- Ferrer J, Malabarba LR (2013) Taxonomic review of the genus *Trichomycterus* Valenciennes (Siluriformes: Trichomycteridae) from the

- laguna dos Patos system, Southern Brazil. *Neotropical Ichthyology* 11: 217–246. <https://doi.org/10.1590/S1679-62252013000200001>
- Katz AM, Barbosa MA (2014) Re-description of *Trichomycterus cubataonis* Bizerril, 1994 (Siluriformes: Trichomycteridae) from the Cubatão river basin, southern Brazil. *Vertebrate Zoology* 64: 3–8.
- Katz AM, Barbosa MA, Mattos JLO, Costa WJEM (2018) Multigene analysis of the catfish genus *Trichomycterus* and description of a new South American trichomycterine genus (Siluriformes, Trichomycteridae). *Zoosystematics and Evolution* 94: 557–566. <https://doi.org/10.3897/zse.94.29872>
- Katz AM, Costa WJEM (2020) A new species of the catfish genus *Cambeva* from the Paranapanema river drainage, southeastern Brazil (Siluriformes: Trichomycteridae). *Tropical Zoology* 33: 2–13. <https://doi.org/10.4081/tz.2020.63>
- Myers N, Mittermeir RA, Mittermeir CG, da Fonseca GAB, Kent J (2000) Biodiversity hotspots for conservation priorities. *Nature* 403: 853–858. <https://doi.org/10.1038/35002501>
- Ochoa LE, Datovo A, DoNascimento C, Roxo FF, Sabaj MH, Chang J, Melo BF, Silva Gabriel SC, Foresti F, Alfaro M, Oliveira C (2020) Phylogenomic analysis of trichomycterid catfishes (Teleostei: Siluriformes) inferred from ultraconserved elements. *Scientific Reports* 10: e2697. <https://doi.org/10.1038/s41598-020-59519-w>
- Ochoa LE, Roxo FF, DoNascimento C, Sabaj MH, Datovo A, Alfaro M, Oliveira C (2017) Multilocus analysis of the catfish family Trichomycteridae (Teleostei: Ostariophysi: Siluriformes) supporting a monophyletic Trichomycterinae. *Molecular Phylogenetics and Evolution* 115: 71–81. <https://doi.org/10.1016/j.ympev.2017.07.007>
- Papavero N (1971) *Essays on the history of Neotropical Dipterology, with special reference to collectors (1750–1905), volume 1*. Museu de Zoologia, Universidade de São Paulo, São Paulo, 2016 pp. <https://doi.org/10.5962/bhl.title.101715>
- Taylor WR, Van Dyke GC (1985) Revised procedures for staining and clearing small fishes and other vertebrates for bone and cartilage study. *Cybium* 9: 107–109. <http://sfi.mnhn.fr/cybium/numeros/1985/92/01-Taylor%5b92%5d107-119.pdf>
- Vilardo PJ, Katz AM, Costa WJEM (2020) Relationships and Description of a New Species of *Trichomycterus* (Siluriformes: Trichomycteridae) from the Rio Paraíba do Sul basin, South-eastern Brazil. *Zoological Studies* 59: e53.
- Wosiacki WB, Oyakawa OT (2005) Two new species of the catfish genus *Trichomycterus* (Siluriformes: Trichomycteridae) from the rio Ribeira de Iguape Basin, Southeastern Brazil. *Neotropical Ichthyology* 3: 465–472. <https://doi.org/10.1590/S1679-62252005000400003>